

Direct current generation by dielectric loss in ferroelectrics

Takahiro Morimoto¹ and Naoto Nagaosa^{2,3}

¹*Department of Applied Physics, The University of Tokyo, Hongo, Tokyo, 113-8656, Japan*

²*RIKEN Center for Emergent Matter Science (CEMS), Wako, Saitama 351-0198, Japan*

³*Fundamental Quantum Science Program, TRIP Headquarters, RIKEN, Wako 351-0198, Japan*

We study direct current (DC) generation induced by microwave irradiation to ferroelectric materials. The DC generation originates from microwave absorption called dielectric loss due to the delay of dielectric response. Such current generation can be formulated as the low-frequency limit of the phonon shift current which arises from an increase of electric polarization accompanying photoexcitation of phonons due to the electron-phonon coupling. To study the DC generation by the dielectric loss, we apply the diagrammatic treatment of nonlinear optical responses to photoexcitations of phonons and derive the general formula for phonon shift current. We then study the DC generation in the low-frequency region and find that the current scales as $\propto \omega^2$ for the linearly polarized light and time reversal symmetric systems. We estimate the order of magnitude of the DC generation by dielectric loss, indicating its feasibility for experimental detection in the GHz region.

I. INTRODUCTION

Ferroelectricity is one of the most fundamental phenomena in solids, where the spontaneous electric polarization is induced by the atomic displacements breaking the spatial inversion symmetry [1]. The simple picture is the separation between the positive and negative charges which results in the electric dipole and the electric polarization P . The modern theory of electronic contribution to the polarization is formulated in terms of the quantum Berry phase of Bloch wave functions [2, 3]. For this formulation, the polarization current j_P associated with the adiabatic change of the atomic positions is the central quantity which is related to the Berry curvature of Bloch electrons. The polarization is defined as the integral of j_P , resulting in Berry phase. Therefore, the ferroelectricity is directly relevant to the geometric nature of the electronic states in solids. In recent years, it has been recognized that the Berry phase is also relevant to the second-order nonlinear optical response to produce the direct current (DC) in noncentrosymmetric materials, i.e., shift current [4–10]. Shift current is induced by the shift of the electronic wave-packet upon interband transition under light irradiation in noncentrosymmetric crystals. Namely, the photoexcited electron-hole pair has nonvanishing electric polarization due to the shift, and a constant increase of the electric polarization in time due to the photoexcitations of electron-hole pairs leads to the DC generation in the steady state. Such shift of electrons can be described by the Berry connection that quantifies the intracell coordinate of Bloch electrons. In this sense, shift current is of a geometric origin and is similar to the polarization current. In particular, it does not originate from the transport of the photo-induced carriers. That said, shift current is still in sharp contrast to the polarization current, in that shift current can be DC whereas the polarization current is always alternating current (AC) under alternating electric fields of electromagnetic waves due to the reversal of the polarization.

Since the shift current does not require the transport of

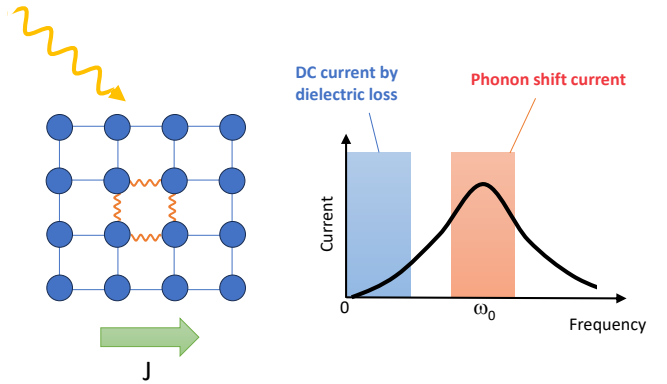


FIG. 1. Schematic picture of direct current (DC) generation by dielectric loss. (Left) Photoexcitation of phonons produces DC in inversion broken materials called phonon shift current, originating from an increase of electric polarization accompanying phonons due to electron-phonon coupling. (Right) In the low frequency region, off resonant phonon excitation leads to dielectric loss in ferroelectrics. According to the shift current mechanism, such dielectric loss also produces DC in the microwave regime.

the photo-induced carriers, it may not require the photo-carriers themselves, i.e., any elementary excitation that accompanies nonzero electric polarization may induce DC generation once such excitation can be photoexcited. This possibility has been explored in the exciton-induced shift current both experimentally and theoretically [11–14]. The photoexcitation of excitons without the external bias voltage induces the DC shift current, where no free charge carriers (i.e., free electrons and holes) exist. In this case, the photocurrent originates from finite electric polarization of excitons where the wave packets of bound electrons and holes are shifted. Even more surprising is the discovery of the shift current in ferroelectric material BaTiO_3 by the phonon excitation at THz region where no electronic excitations take place [15]. The DC emerges by photoexcitation of the phonon which is hybridized with the virtual electron-hole pairs through the

electron-phonon interaction. In ferroelectric materials, such hybridization endows phonons with electric polarization, leading to DC generation with their photoexcitation. Therefore, it is an intriguing issue how the photon energy can be reduced for the shift current generation in insulating materials.

In ferroelectrics, its AC response is described by the dielectric function $\varepsilon(\omega) = \varepsilon'(\omega) + i\varepsilon''(\omega)$. The imaginary part $\varepsilon''(\omega)$ corresponds to the energy dissipation which is proportional to ω in the low frequency limit. This low energy response arises from the delay of the response, i.e., the phase shift, and is extensively studied in the microwave regime, called dielectric loss [16–19].

In the present paper, we study the relation between the phonon-induced shift current and the dielectric loss in the low frequency limit, exploring the possible DC generation associated with the dielectric loss (Fig. 1). To this end, we consider a system of Bloch electrons coupled to phonon excitations as summarized in Sec. II. In Sec. III, using a diagrammatic technique, we derive a general expression for the DC generation that arises from the second order nonlinear response in the external electric field and involves a phonon excitation as an intermediate process. This formulation gives a unified view for the phonon shift current and the DC generation by dielectric loss; the phonon shift current corresponds to the DC generation in the resonant regime ($\omega \simeq \omega_0$ with the phonon frequency ω_0), and the DC generation by the dielectric loss corresponds to the low frequency and off-resonant regime ($\omega \ll \omega_0$), as explained in Sec. IV and Sec. V, respectively. We demonstrate the DC generation in a representative 1D model of ferroelectrics, Rice-Mele model, with a coupling to phonon excitations in Sec. VI, and give an order estimation of the DC generation in the low frequency (\sim GHz) region in Sec. VII, revealing such DC generation is feasible for experimental detection in ferroelectric materials.

II. SETUP

In this section, we present our setup for DC generation, where Bloch electrons in solids are coupled to phonons and subjected to the external electric fields.

We consider the Bloch electrons in solids described by the Hamiltonian,

$$H_{\text{el}} = \sum_{k,a} \varepsilon_a(k) c_{k,a}^\dagger c_{k,a}, \quad (1)$$

with the energy dispersion $\varepsilon_a(k)$ and the annihilation operator of the Bloch electron $c_{k,a}$ for the band a and the momentum k . The coupling to the external electric field

is introduced by the minimal coupling as [20]

$$H_{\text{el-A}} = e \sum_{k,a,b,\alpha} A^\alpha v_{ab}^\alpha(k) c_{k,a}^\dagger c_{k,b} + e^2 \sum_{k,a,b,\alpha,\beta} A^\alpha A^\beta (\partial_{k_\alpha} v^\beta)_{ab}(k) c_{k,a}^\dagger c_{k,b} + O(A^3), \quad (2)$$

where we set $\hbar = 1$ for simplicity. Here, A^α is the vector potential of the electric field along the α direction and we only consider contributions up to $O(A^2)$ as we focus on the second order effect. The velocity operator v^α along the α direction is given by $v^\alpha = \partial_{k_\alpha} H$ when H is represented with k independent basis wave functions. Similarly, the diamagnetic current operator $\partial_{k_\alpha} v^\beta$ is given by $\partial_{k_\alpha} v^\beta = \partial_{k_\alpha} \partial_{k_\beta} H$ in the same representation [10]. In general, one can formulate those current operators as the covariant derivative of the Hamiltonian $v^\alpha = \mathcal{D}^\alpha H$ and that of the velocity operator $\partial_{k_\alpha} H = \mathcal{D}^\alpha H$. Here the covariant derivative \mathcal{D}^α of an operator O is defined with the matrix elements $(\mathcal{D}^\alpha O)_{ab} = \partial_{k_\alpha} O_{ab} - i[\mathcal{A}^\alpha, O]_{ab}$ with the Berry connection $\mathcal{A}^\alpha = i\langle u_a | \partial_{k_\alpha} | u_b \rangle$, where $|u_a\rangle$ is the periodic part of the Bloch wave function of the band a , and the operators with subscripts denote their matrix elements with the Bloch states $O_{ab} = \langle u_a | O | u_b \rangle$. The interband matrix element of the Berry connection is written with a matrix element of the velocity operator as $\mathcal{A}_{ab}^\alpha = -iv_{ab}^\alpha / \varepsilon_{ab}$ with $\varepsilon_{ab} = \varepsilon_a - \varepsilon_b$.

The electron-phonon coupling is given by [21]

$$H_{\text{el-ph}} = \frac{1}{\sqrt{V}} \sum_{k,q,a,b} g_{ab}(k+q, k) c_{k+q,a}^\dagger c_{k,b} (b_q + b_{-q}^\dagger), \quad (3)$$

where V is the total volume of the system, $g_{ab}(k+q, k)$ is the matrix element of the electron phonon coupling in which the electron momentum is modified from k to $k+q$ with the phonon momentum q , $c_{k,a}$ is the annihilation operator of electrons with the momentum k and the band index a , and b_q is the annihilation operator of phonons with the momentum q . The summation runs discrete momenta given by $k = 2\pi n/L$ with the linear dimension L and an integer vector $n \in \mathbb{Z}^3$. Since we consider photoexcitation of phonons, the momentum transfer q is zero. In addition, we further consider the modulation of the electron-phonon coupling $g(k)$ under the electromagnetic field A^α , which is incorporated with a minimal substitution $g(k) \rightarrow g(k) + e \sum_\alpha A^\alpha \partial_{k_\alpha} g(k)$ (where we abbreviated $g_{ab}(k, k)$ by $g_{ab}(k)$). This modulation term $\propto \partial_{k_\alpha} g$ along with the diamagnetic current term in Eq. (2) plays an important role to obtain the correct behavior of the DC generation in the low frequency region avoiding an unphysical divergence. Thus the relevant part of the electron-phonon coupling is given by

$$H_{\text{el-ph}} = \frac{1}{\sqrt{V}} \sum_{k,a,b} [g_{ab}(k) + e \sum_\alpha A^\alpha (\partial_{k_\alpha} g)_{ab}(k)] \times c_{k,a}^\dagger c_{k,b} (b_0 + b_0^\dagger). \quad (4)$$

We note that one may adopt the different notation for the electron-phonon coupling given by

$$H_{\text{el-ph}} = \frac{1}{\sqrt{N}} \sum_{k,q,a,b} \tilde{g}_{ab}(k+q,k) c_{k+q,a}^\dagger c_{k,b} (b_q + b_{-q}^\dagger), \quad (5)$$

where N is the number of unit cells within the system (i.e., $N = V/V_c$ with the unit cell volume V_c). In this notation, \tilde{g} has the dimension of energy and is related to the former notation via $g(k,k') = \sqrt{V_c} \tilde{g}(k,k')$.

III. DC GENERATION WITH PHONONS

In this section, we present the diagrammatic formulation of DC generation by phonon excitations [15]. When the photon energy $\hbar\omega$ is resonant with the phonon energy $\hbar\omega_0$, the real excitation of phonons takes place and leads to DC generation called phonon shift current. When the photon energy $\hbar\omega$ is off resonant with the phonon energy $\hbar\omega_0$, e.g., $\hbar\omega \ll \hbar\omega_0$, the energy dissipation still takes place due to finite energy broadening of the phonon spectrum and results in nonzero DC generation.

A. Diagrammatic derivation of the nonlinear conductivity

We consider DC generation at the second order of the external electric field, which is described by the nonlinear conductivity $\sigma_{\alpha\beta\gamma}(\omega)$ as

$$J_{\text{dc}}^\alpha = \sigma_{\alpha\beta\gamma}(\omega) E^\beta(\omega) E^\gamma(-\omega), \quad (6)$$

where J_{dc}^α is DC along the α direction and $E^\alpha(\omega)$ is the electric field along the α direction of the frequency ω . The nonlinear conductivity $\sigma_{\alpha\beta\gamma}(\omega)$ can be obtained using the standard diagrammatic technique as [20, 21]

$$\sigma_{\alpha\beta\gamma}(\omega) = \frac{e^3}{\omega^2} \Pi_{\alpha\beta\gamma}(\omega), \quad (7)$$

with the response function $\Pi_{\alpha\beta\gamma}$. If we focus on the current generation which arises from the phonon excitations and is in the lowest order in the electron-phonon coupling g , the response function is given by

$$\Pi_{\alpha\beta\gamma}(\omega) = A_1^\beta(\omega) D(\omega) A_2^{\alpha\gamma}(\omega) + A_1^\gamma(-\omega) D(-\omega) A_2^{\alpha\beta}(-\omega), \quad (8)$$

where the diagrammatic representation for the first term is illustrated in Fig. 2(a). Here, $A_1^\beta(\omega)$ represents contributions from diagrams with incoming photon with the frequency ω and outgoing phonon (Fig. 2(b)). The phonon propagator $D(\omega)$ is given by

$$D(\omega) = \frac{2\omega_0}{\omega^2 - \omega_0^2 + 2i\gamma\omega} \simeq \frac{1}{\omega - \omega_0 + i\gamma} - \frac{1}{\omega + \omega_0 + i\gamma}, \quad (9)$$

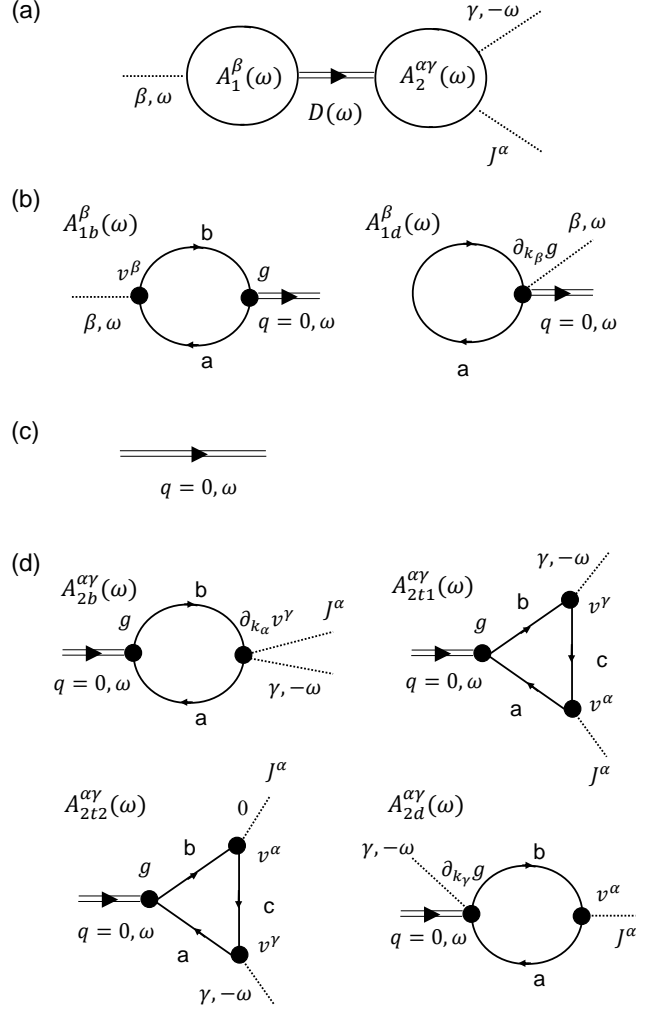


FIG. 2. Diagrams for direct current (DC) generation induced by phonon excitations. (a) The second order nonlinear process responsible for DC generation with phonon excitations. (b) Diagrams $A_1^\beta(\omega)$ with incoming photon with the frequency ω and outgoing phonon. (c) Phonon propagator $D(\omega)$. (d) Diagrams $A_2^{\alpha\gamma}(\omega)$ with incoming phonon, incoming photon with the frequency $-\omega$ and the current vertex.

with the phonon frequency ω_0 and the energy broadening for the phonon γ (Fig. 2(c)) [22]. $A_2^{\alpha\gamma}(\omega)$ represents contributions from the diagrams with incoming phonon, incoming photon with the frequency $-\omega$ and the current vertex (Fig. 2(d)).

To compute contributions from the diagrams, we adopt the imaginary time formalism for Green's function. For simplicity, we focus on the zero temperature case, where the Green's function in the Matsubara frequency representation is given by

$$G(k, i\omega) = \sum_a \frac{|u_a\rangle \langle u_a|}{i\omega - \epsilon}. \quad (10)$$

We consider two incoming photons with Matsubara fre-

quencies $i\Omega_1$ and $i\Omega_2$ that are analytically continued as

$$i\Omega_1 \rightarrow \omega + i\gamma', \quad i\Omega_2 \rightarrow -\omega + i\gamma', \quad (11)$$

with the photon frequency ω and the relaxation strength γ' . Below, we assume the relaxation strength γ' is much smaller than the band separation of electrons, and we neglect γ' . The first bubble diagram A_{1b}^β is given by

$$\begin{aligned} A_{1b}^\beta(i\Omega_1) &= \int \frac{d\omega}{2\pi} \int [dk] \text{Tr}[gG(k, i\omega + i\Omega_1)v^\beta G(k, i\omega)] \\ &= \int \frac{d\omega}{2\pi} \int [dk] \sum_{ab} g_{ab} \frac{1}{i\omega + i\Omega_1 - \epsilon_a} v_{ba}^\beta \frac{1}{i\omega - \epsilon_a} \\ &= \int [dk] \sum_{ab} \frac{f_{ab}g_{ab}v_{ba}^\beta}{i\Omega_1 - \epsilon_{ba}}. \end{aligned} \quad (12)$$

Here we use the notation $\int [dk] \equiv \int d^d k / (2\pi)^d$, ϵ_a and f_a are the energy and the Fermi distribution function for the state a , respectively. We also use the notations: $f_{ab} = f_a - f_b$ and $\epsilon_{ab} = \epsilon_a - \epsilon_b$. In addition, we have a contribution A_{1d}^β arising from modulation of electron-phonon coupling g in the presence of the electric field, which is described by the vertex $\partial_k g$ in a similar manner to the diamagnetic current (Fig. 2(b)). This contribution is important to derive correct behavior of the response function in the low frequency region, avoiding unphysical divergence that arises from $1/\omega^2$ factor in Eq. (7). Specifically, this contribution reads

$$\begin{aligned} A_{1d}^\beta(i\Omega_1) &= \int \frac{d\omega}{2\pi} \int [dk] \text{Tr}[\partial_{k_\beta} g G(k, i\omega)] \\ &= - \int \frac{d\omega}{2\pi} \int [dk] \text{Tr}[gG(k, i\omega)v^\beta G(k, i\omega)] \\ &= -A_{1b}^\beta(0). \end{aligned} \quad (13)$$

Combining these two contributions and performing the analytic continuation $i\Omega_1 \rightarrow \omega$ and writing $\tilde{A}_1^\beta = A_{1b}^\beta / \omega$, we obtain

$$\begin{aligned} \tilde{A}_1^\beta(\omega) &= \frac{1}{\omega} (A_{1b}^\beta(\omega) + A_{1d}^\beta(\omega)) \\ &= \int [dk] \sum_{ab} \frac{1}{\epsilon_{ba}} \frac{f_{ab}g_{ab}v_{ba}^\beta}{\omega - \epsilon_{ba}}, \end{aligned} \quad (14)$$

by using the identity,

$$\frac{1}{\omega} \left(\frac{1}{\omega - x} - \frac{1}{-x} \right) = \frac{1}{x(\omega - x)}. \quad (15)$$

The second bubble diagram $A_2^{\alpha\gamma}$ has three contributions: a bubble diagram made of diamagnetic current vertex $A_{2b}^{\alpha\gamma}$, a triangle diagram involving two (paramagnetic) current vertices $A_{2t}^{\alpha\gamma}$, and a bubble diagram $A_{2d}^{\alpha\gamma}$

involving $\partial_k g$. The diagram $A_{2b}^{\alpha\gamma}$ can be computed in a similar manner as A_1^β and is given by

$$\begin{aligned} A_{2b}^{\alpha\gamma}(i\Omega_1) &= \int \frac{d\omega}{2\pi} \int [dk] \text{Tr}[\partial_{k_\alpha} v^\gamma G(k, i\omega + i\Omega_1)gG(k, i\omega)] \\ &= \int [dk] \sum_{ab} \frac{f_{ab}(\partial_{k_\alpha} v^\gamma)_{ab}g_{ba}}{i\Omega_1 - \epsilon_{ba}}. \end{aligned} \quad (16)$$

The diagram $A_{2t}^{\alpha\gamma}$ can be further separated into two pieces $A_{2t1}^{\alpha\gamma}$ and $A_{2t2}^{\alpha\gamma}$ according to the order of the other incoming photon and the current vertex. The contributions $A_{2t1}^{\alpha\gamma}$ is given by

$$\begin{aligned} A_{2t1}^{\alpha\gamma}(i\Omega_1) &= \int \frac{d\omega}{2\pi} \int [dk] \text{Tr}[v^\alpha G(k, i\omega + i\Omega_1 + i\Omega_2) \\ &\quad \times v^\gamma G(k, i\omega + i\Omega_1)gG(k, i\omega)] \\ &= \int [dk] \sum_{a,b,c} v_{ac}^\alpha v_{cb}^\gamma g_{ba} I_{abc}(i\Omega_1, i\Omega_2), \end{aligned} \quad (17)$$

with

$$\begin{aligned} I_{abc}(i\Omega_1, i\Omega_2) &= \int \frac{d\omega}{2\pi} \frac{1}{(i\omega + i\Omega_1 + i\Omega_2 - \epsilon_c)(i\omega + i\Omega_1 - \epsilon_b)(i\omega - \epsilon_a)} \\ &= \frac{1}{\epsilon_{ac} + i\Omega_1 + i\Omega_2} \left(\frac{f_{ab}}{i\Omega_1 - \epsilon_{ba}} - \frac{f_{cb}}{-i\Omega_2 - \epsilon_{bc}} \right). \end{aligned} \quad (18)$$

Similarly, the contributions $A_{2t2}^{\alpha\gamma}$ is given by

$$\begin{aligned} A_{2t2}^{\alpha\gamma}(i\Omega_1) &= \int \frac{d\omega}{2\pi} \int [dk] \text{Tr}[v^\gamma G(k, i\omega - i\Omega_2)v^\alpha G(k, i\omega + i\Omega_1)gG(k, i\omega)] \\ &= \int [dk] \sum_{a,b,c} v_{bc}^\gamma v_{ca}^\alpha g_{ab} I_{bac}(i\Omega_1, -i\Omega_1 - i\Omega_2) \\ &= \int [dk] \sum_{a,b,c} (v_{ac}^\alpha v_{cb}^\gamma g_{ba})^* I_{abc}(-i\Omega_1, -i\Omega_2), \end{aligned} \quad (19)$$

where we changed the variable as $i\omega \rightarrow i\omega - i\Omega_1$ in the integral I in the last line. In addition, the contribution from $A_{2d}^{\alpha\gamma}$ that involves $\partial_k g$ reads

$$\begin{aligned} A_{2d}^{\alpha\gamma}(i\Omega_1) &= \int \frac{d\omega}{2\pi} \int [dk] \text{Tr}[v^\gamma G(k, i\omega)\partial_{k_\alpha} g G(k, i\omega)] \\ &= - \int \frac{d\omega}{2\pi} \int [dk] \text{Tr}[\partial_{k_\alpha} v^\gamma G(k, i\omega)gG(k, i\omega) \\ &\quad + v^\alpha G(k, i\omega)v^\gamma G(k, i\omega)gG(k, i\omega) \\ &\quad + v^\gamma G(k, i\omega)v^\alpha G(k, i\omega)gG(k, i\omega)], \\ &= -(A_{2b}(0) + A_{2t1}(0) + A_{2t2}(0)), \end{aligned} \quad (20)$$

which correctly cancels the low frequency divergences of A_{2b} , A_{2t1} , and A_{2t2} .

Thus after the analytic continuation of Matsubara frequencies and writing $A_2^{\alpha\gamma} = A_2^{\alpha\gamma}/\omega$, we obtain

$$\begin{aligned}\tilde{A}_2^{\alpha\gamma}(\omega) &= \frac{1}{\omega}(A_{2b}^{\alpha\gamma}(\omega) + A_{2t1}^{\alpha\gamma}(\omega) + A_{2t2}^{\alpha\gamma}(\omega) + A_{2d}^{\alpha\gamma}(\omega)) \\ &= \int [dk] \sum_{ab} \frac{f_{ab}(\partial_{k_\alpha} v^\gamma)_{ab} g_{ba}}{\epsilon_{ba}(\omega - \epsilon_{ba})} \\ &\quad + \int [dk] \sum_{abc} v_{ac}^\alpha v_{cb}^\gamma g_{ba} \frac{1}{\epsilon_{ac}} \left(\frac{f_{ab}}{\epsilon_{ba}(\omega - \epsilon_{ba})} - \frac{f_{cb}}{\epsilon_{bc}(\omega - \epsilon_{bc})} \right) \\ &\quad + \int [dk] \sum_{abc} (v_{ac}^\alpha v_{cb}^\gamma g_{ba})^* \frac{1}{\epsilon_{ac}} \left(-\frac{f_{ab}}{\epsilon_{ba}(-\omega - \epsilon_{ba})} + \frac{f_{cb}}{\epsilon_{bc}(-\omega - \epsilon_{bc})} \right).\end{aligned}\quad (21)$$

The DC that can be extracted out of the system inevitably accompanies energy dissipation in the system. In the present case, such energy dissipation arises from the phonon excitation and is described by the imaginary part of the phonon propagator $\text{Im}[D(\omega)]$. Thus, focusing on the contributions that involve $\text{Im}[D(\omega)]$, we obtain the general expression for the DC generation with phonon excitations as

$$\sigma_{\alpha\beta\gamma}(\omega) = -e^3 C_{\alpha\beta\gamma}(\omega) \text{Im}[D(\omega)], \quad (22)$$

with

$$C_{\alpha\beta\gamma}(\omega) = \text{Im} \left[\tilde{A}_1^\beta(\omega) \tilde{A}_2^{\alpha\gamma}(\omega) - \tilde{A}_1^\gamma(-\omega) \tilde{A}_2^{\alpha\beta}(-\omega) \right]. \quad (23)$$

B. Role of time reversal symmetry

Next let us consider the role of the time reversal symmetry \mathcal{T} on the nonlinear conductivity $\sigma_{\alpha\beta\gamma}(\omega)$. When the system preserves \mathcal{T} , the energy dispersion is k -even as

$$\epsilon_a(k) = \epsilon_a(-k), \quad (24)$$

and the matrix elements of the velocity operator v , the diamagnetic current $\partial_k v$ and the electron-phonon coupling g satisfy the following relationships,

$$\begin{aligned}v_{ab}(k) &= -v_{ba}(-k), \\ (\partial_k v)_{ab}(k) &= (\partial_k v)_{ba}(-k), \\ g_{ab}(k) &= g_{ba}(-k).\end{aligned}\quad (25)$$

Note that the Bloch states $u_a(\pm k)$ are Kramers pairs for cases with spin orbit couplings. With these symmetry properties, \tilde{A}_1^β becomes purely imaginary and $\tilde{A}_2^{\alpha\gamma}$ becomes purely real. Expanding \tilde{A}_1^β and $\tilde{A}_2^{\alpha\gamma}$ with respect to ω gives

$$\begin{aligned}\tilde{A}_1^\beta &= -i \int [dk] \sum_{ab} \text{Im}[g_{ab} v_{ba}^\beta] \frac{f_{ab}}{\epsilon_{ba}^2} \\ &\quad - i\omega \int [dk] \sum_{ab} \text{Im}[g_{ab} v_{ba}^\beta] \frac{f_{ab}}{\epsilon_{ba}^3} + O(\omega^2),\end{aligned}\quad (26)$$

and

$$\begin{aligned}\tilde{A}_2^{\alpha\gamma} &= - \int [dk] \sum_{ab} \text{Re}[(\partial_{k_\alpha} v^\gamma)_{ab} g_{ba}] \frac{f_{ab}}{\epsilon_{ba}^2} \\ &\quad - \omega \int [dk] \sum_{ab} \text{Re}[(\partial_{k_\alpha} v^\gamma)_{ab} g_{ba}] \frac{f_{ab}}{\epsilon_{ba}^3} \\ &\quad - 2\omega \int [dk] \sum_{abc} \text{Re}[v_{ac}^\alpha v_{cb}^\gamma g_{ba}] \frac{1}{\epsilon_{ac}} \left(\frac{f_{ab}}{\epsilon_{ba}^3} - \frac{f_{cb}}{\epsilon_{bc}^3} \right) \\ &\quad + O(\omega^2).\end{aligned}\quad (27)$$

For the case of linearly polarized light $\beta = \gamma$ and the ab-initio Hamiltonian for electrons $H = p^2/2m + V(r)$ where $(\partial_k v)_{ab} = 0$ holds for $a \neq b$, the coefficient $C_{\alpha\beta\gamma}(\omega)$ for the nonlinear conductivity Eq.(22) is given by

$$\begin{aligned}C_{\alpha\beta\beta}(\omega) &= 4\omega \left\{ \int [dk] \sum_{ab} \text{Im}[g_{ab} v_{ba}^\beta] \frac{f_{ab}}{\epsilon_{ba}^2} \right\} \\ &\quad \times \left\{ \int [dk] \sum_{abc} \text{Re}[v_{ac}^\alpha v_{cb}^\beta g_{ba}] \frac{1}{\epsilon_{ac}} \left(\frac{f_{ab}}{\epsilon_{ba}^3} - \frac{f_{cb}}{\epsilon_{bc}^3} \right) \right\},\end{aligned}\quad (28)$$

in the least order in ω . In general, the coefficient $C_{\alpha\beta\beta}(\omega)$ is proportional to ω in the presence of \mathcal{T} .

IV. PHONON SHIFT CURRENT

Let us consider the incoming photon frequency is resonant to the phonon frequency, $\omega \simeq \omega_0$, to study phonon shift current. In this case, we replace $D(\omega)$ by the delta function as

$$D(\omega) \simeq -i\pi[\delta(\omega - \omega_0) - \delta(\omega + \omega_0)]. \quad (29)$$

Using Eq. (22) for the nonlinear conductivity, we obtain the formula for the phonon shift current as

$$\begin{aligned}\sigma_{\alpha\beta\gamma}(\omega) &\simeq \pi e^3 \text{Im} \left[\tilde{A}_1^\beta(\omega) \tilde{A}_2^{\alpha\gamma}(\omega) - \tilde{A}_1^\gamma(-\omega) \tilde{A}_2^{\alpha\beta}(-\omega) \right] \\ &\quad \times \delta(\omega - \omega_0),\end{aligned}\quad (30)$$

with \tilde{A}_1 and \tilde{A}_2 in Eq. (14) and Eq. (21).

For the case of linearly polarized light and the ab-initio Hamiltonian, the expression for the phonon shift current is given by

$$\begin{aligned} \sigma_{\alpha\beta\beta}(\omega) &= 4\pi e^3 \omega \left\{ \int [dk] \sum_{ab} \text{Im}[g_{ab} v_{ba}^\beta] \frac{f_{ab}}{\epsilon_{ba}^2} \right\} \\ &\times \left\{ \int [dk] \sum_{abc} \text{Re}[v_{ac}^\alpha v_{cb}^\beta g_{ba}] \frac{1}{\epsilon_{ac}} \left(\frac{f_{ab}}{\epsilon_{ba}^3} - \frac{f_{cb}}{\epsilon_{bc}^3} \right) \right\} \\ &\times \delta(\omega - \omega_0). \end{aligned} \quad (31)$$

This formula clearly indicates that photoexcitations of phonons, which are charge neutral and usually lie much below the electronic band gap, can produce dc charge current generation. Such charge current is essentially induced by the shift current mechanism since the phonons in noncentrosymmetric crystals accompany nonzero electric polarization.

V. DIRECT CURRENT FROM DIELECTRIC LOSS

In this section, we consider DC generation arising from dielectric loss in ferroelectrics with off resonant driving in the low frequency region ($\omega \ll \omega_0$).

We start with the expression for the DC generation in Eq. (22). The presence of the imaginary part of the phonon propagator $\text{Im}[D(\omega)]$ in Eq. (22) describes the energy dissipation due to the phonons, which corresponds to the dielectric loss in the low frequency region. Thus the formula Eq. (22) indicates that the dielectric loss can generally induce the DC generation through shift current mechanism. The imaginary part of the phonon propagator reads

$$\begin{aligned} \text{Im}[D(\omega)] &= \frac{-4\omega_0\gamma\omega}{(\omega^2 - \omega_0^2)^2 + (2\gamma\omega)^2} \\ &\simeq -4\frac{\gamma\omega}{\omega_0^3}, \quad (\omega \ll \omega_0) \end{aligned} \quad (32)$$

in the low frequency region. Thus the nonlinear conductivity in the low frequency region is given by

$$\sigma_{\alpha\beta\gamma}(\omega) = \frac{4e^3\gamma\omega}{\omega_0^3} C_{\alpha\beta\gamma}(\omega), \quad (33)$$

with the coefficient $C_{\alpha\beta\gamma}(\omega)$ in Eq. (23). For the time reversal symmetric systems under linearly polarized light $\beta = \gamma$, the nonlinear conductivity scales as

$$\sigma_{\alpha\beta\beta}(\omega) \propto \omega^2, \quad (\omega \ll \omega_0) \quad (34)$$

because of $C_{\alpha\beta\beta}(\omega) \propto \omega$. This behavior is reasonable in that the current should vanish in an insulator with the adiabatic limit ($\omega \rightarrow 0$), since the electric polarization adiabatically follows the external electric field for $\omega \rightarrow 0$. In addition, one can interchange $\omega \leftrightarrow -\omega$ in Eq. (6) for linearly polarized light $\beta = \gamma$, indicating

that $\sigma_{\alpha\beta\beta}(\omega)$ is an even function of ω . Combining these two properties leads to the scaling $\sigma_{\alpha\beta\beta}(\omega) \propto \omega^2$ in the low frequency region. In contrast, for circularly polarized light ($\beta \neq \gamma$), $\omega \leftrightarrow -\omega$ is not interchangeable in Eq. (6), indicating the ω linear term in $\sigma_{\alpha\beta\gamma}(\omega)$ is allowed.

In comparison, at the phonon resonance $\omega = \omega_0$, the DC generation under the linearly polarized light is given by

$$\sigma_{\alpha\beta\beta}(\omega_0) = \frac{e^3}{\gamma} C_{\alpha\beta\beta}(\omega_0), \quad (35)$$

with $\text{Im}[D(\omega_0)] = 1/\gamma$. Thus the ratio of the DC generation associated with dielectric loss to the phonon shift current is given by

$$\frac{\sigma_{\alpha\beta\beta}(\omega)}{\sigma_{\alpha\beta\beta}(\omega_0)} \simeq \frac{4\gamma^2\omega}{\omega_0^3} \frac{C_{\alpha\beta\beta}(\omega)}{C_{\alpha\beta\beta}(\omega_0)} = \frac{4\gamma^2\omega^2}{\omega_0^4}, \quad (36)$$

in the low frequency region, $\omega \ll \omega_0$.

To discuss the amount of the DC in the present mechanism incorporating the effect of the absorption depth, it is good to look at the Glass coefficient which is defined by

$$G_{\alpha\beta\beta}(\omega) = \frac{J_{\text{dc}}^\alpha}{\alpha_{\text{abs}} I_\beta}, \quad (37)$$

with the absorption coefficient α_{abs} and the intensity of the incident light I_β with linear polarization along the β direction [23, 24]. The absorption coefficient α_{abs} is proportional to the linear conductivity $\sigma_{\beta\beta}(\omega)$, which scales linearly in ω , if we neglect relaxation mechanisms other than the phonon excitations. This ω linear scaling of $\sigma_{\beta\beta}(\omega)$ can be derived from

$$\sigma_{\beta\beta}(\omega) = -e^2 \left\{ \tilde{A}_1^\beta(\omega) \text{Im}[D(\omega)] [A_{1b}^\beta(\omega)]^* + (\omega \leftrightarrow -\omega) \right\}, \quad (38)$$

where $\tilde{A}_1^\beta(\omega) [A_{1b}^\beta(\omega)]^* \rightarrow \text{const.}$ and $\text{Im}[D(\omega)] \propto \omega$ for $\omega \ll \omega_0$. Thus the Glass coefficient behaves as

$$G(\omega) \propto \frac{\sigma_{\alpha\beta\beta}(\omega)}{\sigma_{\beta\beta}(\omega)} \propto \omega, \quad (39)$$

in the low frequency region.

VI. APPLICATION TO RICE-MELE MODEL

In this section, we demonstrate the DC generation by dielectric loss by applying our formulation to a model of ferroelectrics. Specifically, we consider Rice-Mele model which is a representative model of 1D ferroelectrics and is described by the Hamiltonian given by

$$H_{RM} = \sum_k \Psi_k^\dagger \left(t \cos \frac{ka}{2} \sigma_x + \delta t \sin \frac{ka}{2} \sigma_y + m \sigma_z \right) \Psi_k, \quad (40)$$

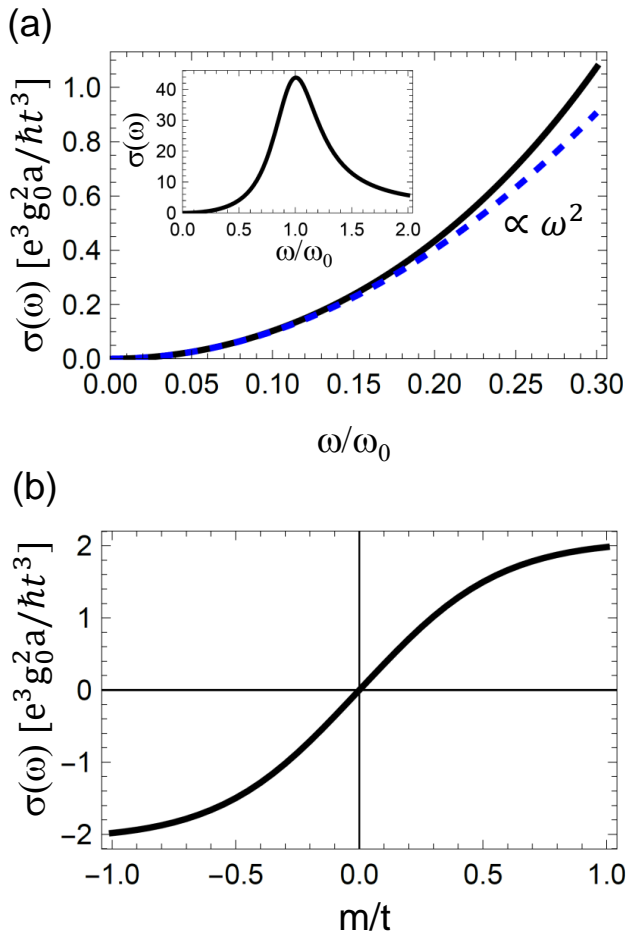


FIG. 3. DC generation in Rice-Mele model coupled with phonons. (a) Nonlinear conductivity $\sigma(\omega)$ in the low frequency regime below the phonon excitation. Blue dashed curve is a fit of $\sigma(\omega)$ with a form $C\omega^2$ indicating the scaling of $\sigma(\omega) \propto \omega^2$. Inset shows $\sigma(\omega)$ in the phonon resonance region $\omega \sim \omega_0$ corresponding to the phonon shift current. (b) Staggered potential (m) dependence of nonlinear conductivity $\sigma(\omega)$. $\sigma(\omega)$ at the fixed frequency, $\omega = 0.25\omega_0$, shows a sign change with respect to the sign of m , indicating that the current direction switches depending on the direction of the electric polarization. We adopted the parameters, $\delta t/t = 0.2, \omega_0/\omega = 0.2, \gamma/t = 0.05$ for (a) and (b), and $m/t = 0.2$ for (a).

with

$$\Psi_k = \begin{pmatrix} c_{A,k} \\ c_{B,k} \end{pmatrix}, \quad (41)$$

where t is the hopping amplitude, δt is the strength of hopping alternation, m is the strength of staggered potential, a is the lattice constant, and σ_i is the Pauli matrix acting on sublattice (AB) degrees of freedom. We consider an electron-phonon coupling in the form of

Eq. (4) with

$$g(k) = g_0 \sin \frac{ka}{2} \sigma_y, \quad (42)$$

where the phonon excitation modulates the bond alternation with the strength g_0 .

In this setup, the diagrams constituting DC generation in Fig. 2 can be evaluated with Eq. (14) and Eq. (21). We show the result of numerical calculation in Fig. 3 for the parameters. Figure 3(a) shows the nonlinear conductivity $\sigma(\omega)$ in the low frequency regime below the phonon excitation, where DC generation by the dielectric loss takes place. In the low frequency region, $\sigma(\omega)$ scales as $\propto \omega^2$ as indicated by a ω^2 fit in the blue dashed curve. The inset shows a behavior of $\sigma(\omega)$ in the phonon resonance region $\omega \sim \omega_0$ which corresponds to the phonon shift current. The nonlinear conductivity $\sigma(\omega)$ at fixed ω shows a sign change with respect to the sign of the staggered potential m as shown in Fig. 3(b). Since m determines the pattern of the inversion symmetry breaking and the direction of the electric polarization, this sign change of $\sigma(\omega)$ indicates that the direction of the DC generation is governed by the direction of the electric polarization.

VII. DISCUSSION

Berry phase was originally formulated for the adiabatic process, where the transitions of wavefunction between the different energy eigenstates are forbidden [25]. Therefore, its application to solids is naively considered to be limited to the low energy phenomena where the interband transitions are forbidden, i.e., the wavefunctions are confined within the manifold spanned by the states specified by the band index [26]. On the other hand, the shift current due to the interband transition is formulated by the Berry connections of Bloch wavefunctions, where the adiabatic approximation is never justified. In the case of the shift current due to phonon excitation, there is no real transitions of electrons between bands; instead the virtual transition of electrons that accompanies the real excitation of phonons induces the DC. Thus, it appears to be an “adiabatic” process for electronic degrees of freedom. However, from the viewpoint of the Born-Oppenheimer approximation (BOA) [27], which is the adiabatic approximation based on the difference in the time-scales of electrons and phonons, the nonadiabatic corrections to BOA is the origin of the shift current. This is especially clear in the present dielectric loss, in that the small but finite frequency gives the absorption and shift current simultaneously. Also, the existence of energy supply is crucial for shift current responses to support the DC generation in non-superconducting system even though it is of a geometric origin.

Note that, in real materials, the dielectric loss could occur also due to the motion of the domain walls. In this case, the generation of the shift current is localized in the

domain wall regions, and has the opposite signs between the two types of the domain wall, i.e., (+, -) and (-, +).

Lastly, we present an estimation for the DC generation from dielectric loss. For soft phonon excitations in BaTiO₃ studied in Ref. [15], photocurrent of the order of 10 μ A with the Glass coefficient $G \simeq 1 \times 10^{-8}$ cm/V has been observed. For soft phonons (e.g., Slater mode in BaTiO₃), the typical values for the phonon frequency and the energy broadening are given by $\omega_0 \simeq 4$ meV and $\gamma \simeq 4$ meV [15]. If one considers the dielectric loss in the presence of AC electric field in the off-resonant gigahertz regime, e.g., $\omega = 10$ GHz, the ratio of the nonlinear conductivities $\sigma_{\alpha\beta\beta}(\omega)/\sigma_{\alpha\beta\beta}(\omega_0)$ is given by $4\gamma^2\omega^2/\omega_0^4 \simeq 4 \times 10^{-4}$. Since the nonlinear conductivity of $\sigma_{\alpha\beta\beta}(\omega_0) \simeq 30 \mu\text{A}/\text{V}^2$ is reported in ab-initio calculation [15], we expect $\sigma_{\alpha\beta\beta}(\omega) \simeq 0.01 \mu\text{A}/\text{V}^2$ for

$\omega = 10$ GHz. For the electric field of $E = 1$ kV/cm and the sample dimension of $d = 0.1$ mm, the DC generation of 1 μ A is expected from dielectric loss, which is feasible for experimental detection. For the Glass coefficient, we expect $G \simeq 1 \times 10^{-10}$ cm/V for $\omega = 10$ GHz from the measured value for the phonon shift current, $G \simeq 1 \times 10^{-8}$ cm/V for $\omega = 1$ THz.

ACKNOWLEDGMENTS

We thank N. Ogawa, K. Kanoda and Y. Tokura for fruitful discussions. This work was supported by JSPS KAKENHI Grant 23H01119, 23K17665 (T.M.), and JST CREST (Grant No. JPMJCR19T3) (T.M.).

-
- [1] M. E. Lines and A. M. Glass, *Principles and applications of ferroelectrics and related materials* (Oxford university press, 2001).
- [2] R. Resta, Macroscopic polarization in crystalline dielectrics: the geometric phase approach, *Rev. Mod. Phys.* **66**, 899 (1994).
- [3] R. D. King-Smith and D. Vanderbilt, Theory of polarization of crystalline solids, *Phys. Rev. B* **47**, 1651 (1993).
- [4] R. von Baltz and W. Kraut, Theory of the bulk photovoltaic effect in pure crystals, *Phys. Rev. B* **23**, 5590 (1981).
- [5] J. E. Sipe and A. I. Shkrebtii, Second-order optical response in semiconductors, *Phys. Rev. B* **61**, 5337 (2000).
- [6] S. M. Young and A. M. Rappe, First principles calculation of the shift current photovoltaic effect in ferroelectrics, *Phys. Rev. Lett.* **109**, 116601 (2012).
- [7] T. Morimoto and N. Nagaosa, Topological nature of nonlinear optical effects in solids, *Science Advances* **2**, e1501524 (2016).
- [8] A. M. Cook, B. M. Fregoso, F. De Juan, S. Coh, and J. E. Moore, Design principles for shift current photovoltaics, *Nature communications* **8**, 14176 (2017).
- [9] Z. Dai and A. M. Rappe, Recent progress in the theory of bulk photovoltaic effect, *Chemical Physics Reviews* **4**, 011303 (2023).
- [10] T. Morimoto, S. Kitamura, and N. Nagaosa, Geometric aspects of nonlinear and nonequilibrium phenomena, *Journal of the Physical Society of Japan* **92**, 072001 (2023), <https://doi.org/10.7566/JPSJ.92.072001>.
- [11] T. Morimoto and N. Nagaosa, Topological aspects of nonlinear excitonic processes in noncentrosymmetric crystals, *Phys. Rev. B* **94**, 035117 (2016).
- [12] M. Sotome, M. Nakamura, T. Morimoto, Y. Zhang, G.-Y. Guo, M. Kawasaki, N. Nagaosa, Y. Tokura, and N. Ogawa, Terahertz emission spectroscopy of ultrafast exciton shift current in the noncentrosymmetric semiconductor cds, *Phys. Rev. B* **103**, L241111 (2021).
- [13] Y.-H. Chan, D. Y. Qiu, F. H. da Jornada, and S. G. Louie, Giant exciton-enhanced shift currents and direct current conduction with sub-bandgap photo excitations produced by many-electron interactions, *Proceedings of the National Academy of Sciences* **118**, e1906938118 (2021), <https://www.pnas.org/doi/pdf/10.1073/pnas.1906938118>.
- [14] T. Akamatsu, T. Ideue, L. Zhou, Y. Dong, S. Kitamura, M. Yoshii, D. Yang, M. Onga, Y. Nakagawa, K. Watanabe, T. Taniguchi, J. Laurienzo, J. Huang, Z. Ye, T. Morimoto, H. Yuan, and Y. Iwasa, A van der waals interface that creates in-plane polarization and a spontaneous photovoltaic effect, *Science* **372**, 68 (2021).
- [15] Y. Okamura, T. Morimoto, N. Ogawa, Y. Kaneko, G.-Y. Guo, M. Nakamura, M. Kawasaki, N. Nagaosa, Y. Tokura, and Y. Takahashi, Photovoltaic effect by soft phonon excitation, *Proceedings of the National Academy of Sciences* **119**, e2122313119 (2022).
- [16] V. Gurevich and A. Tagantsev, Intrinsic dielectric loss in crystals, *Advances in Physics* **40**, 719 (1991).
- [17] M. Sparks, D. F. King, and D. L. Mills, Simple theory of microwave absorption in alkali halides, *Phys. Rev. B* **26**, 6987 (1982).
- [18] K. R. Subbaswamy and D. L. Mills, Theory of microwave absorption in wide-band-gap insulators: The role of thermal phonon lifetimes, *Phys. Rev. B* **33**, 4213 (1986).
- [19] X. Aupi, J. Breeze, N. Ljepojevic, L. J. Dunne, N. Malde, A.-K. Axelsson, and N. M. Alford, Microwave dielectric loss in oxides: Theory and experiment, *Journal of applied physics* **95**, 2639 (2004).
- [20] D. E. Parker, T. Morimoto, J. Orenstein, and J. E. Moore, Diagrammatic approach to nonlinear optical response with application to weyl semimetals, *Phys. Rev. B* **99**, 045121 (2019).
- [21] G. D. Mahan, *Many Particle Physics, Third Edition* (Plenum, New York, 2000).
- [22] J. F. Scott, Soft-mode spectroscopy: Experimental studies of structural phase transitions, *Rev. Mod. Phys.* **46**, 83 (1974).
- [23] A. Glass, D. v. d. Linde, and T. Negran, High-voltage bulk photovoltaic effect and the photorefractive process in LiNbO₃, *Appl. Phys. Lett.* **25**, 233 (1974).
- [24] G. B. Osterhoudt, L. K. Diebel, M. J. Gray, X. Yang, J. Stanco, X. Huang, B. Shen, N. Ni, P. J. Moll, Y. Ran, *et al.*, Colossal mid-infrared bulk photovoltaic effect in a type-I Weyl semimetal, *Nature materials* **18**, 471 (2019).

- [25] M. V. Berry, Geometric amplitude factors in adiabatic quantum transitions, *Proc. Roy. Soc. London A* **430**, 405 (1990).
- [26] D. Xiao, M.-C. Chang, and Q. Niu, Berry phase effects on electronic properties, *Rev. Mod. Phys.* **82**, 1959 (2010).
- [27] C. A. Mead, The geometric phase in molecular systems, *Rev. Mod. Phys.* **64**, 51 (1992).